CONFIGURATION OF L-BAND POLARIMETRIC SIGNATURES AND SCATTERING MECHANISMS OF FOREST TARGETS IN THE BRAZILIAN AMAZON

J. R. dos Santos[a] ; F. G. Gonçalves[b]

[a]INPE , National Institute for Space Research,
Av. dos Astronautas, 1758 CEP.:12.227-010 São José dos Campos – SP., Brazil - jroberto@ltid.inpe.br
[b]Department of Forest Science, Oregon State University, Corvallis, OR 97331, EUA - Fabio.Goncalves@oregonstate.edu

Commission VIII, WG VIII/11

KEYWORDS: Forestry,Land cover, SAR, Inventory, Monitoring, Recognition.

ABSTRACT:

The objective of this study is to analyze the graphic representation of polarimetric signatures of airborne SAR-R99B data (L-band) in primary forest, secondary successions, forest with timber exploitation and those under recovery after a surface burning process. Additionally, another objective is an exploratory analysis of scattering mechanisms of forest typology in accordance with the alternative procedure of SAR image classification based on target decomposition. The area under study is located at the Tapajós region (Brazil). At the representation of polarimetric signatures, the normalized cross-section of the forest target (σ) was plotted on a three-dimensional graphic as a function of the orientation angle, ellipticity angle, referring to the ellipse of polarization. The resulting surfaces were visually compared and the configuration of each plot was analyzed with support of physiognomic-structural information collected during forest inventories. On the other hand, the distinction between simple and multiple scattering mechanism from the target decomposition was done by the association of entropy and alpha angle values for each sample area. Some results can be mentioned: (a) from the analysis of polarimetric signatures one can verify that the primary forest sections present a relatively high pedestal when compared to the secondary succession. (b) for all thematic classes studied the pixel distribution in the (H, α) bi-dimensional space was more frequent at zones 5, 4 and 6 (decreasing frequency order). This study improves the understanding of the interaction mechanisms between L-band SAR signals and structural parameters of tropical rainforest, subsidizing the inventory and the monitoring of land cover in the Amazon region.

1 INTRODUCTION

Due to the advancement of economic activities in the domain of the Amazon tropical rainforest, remote sensing is becoming a fundamental tool to characterize the causes of degradation (conversion of natural vegetation to agriculture and cattle raising, selective logging, charcoal production, etc.) but also to monitor the impact of human activities (fragmentation of habitats; loss of biodiversity; reduction of hydrological and edaphic potentials) over these large ecosystems. Taking into account that in tropical regions there is, all over the year, a high percentage of cloud cover which impedes the inventory and updating of the forest cover by optical data, it is important to use sensor systems which operate at microwave wavelengths.

Rauste et al. (1994) and Henderson & Lewis (1998), who studied the multi-polarimetric SAR backscatter for the discrimination of forest types, discussing those aspects of scattering and attenuation of the SAR signal at different frequencies. Furthermore, Kugler et al. (2006) and Treuhaft et al. (2006) discuss the contribution of the interferometric SAR mode to estimate biophysical parameters in forest areas. Power spectrum analysis was used for the analysis of spatial forest features (canopy structure and distances between major tree individuals) from airborne SAR data in the Brazilian Amazon (Neeff et al., 2005). Saatchi et al. (1997), Hoekman and Quiñones (2000), Santos et al. (2003), estimated specifically the forest biomass by polarimetric and/or interferometric SAR data, discussing the backscatter saturation due to the high density of tropical forests. These above mentioned experiments indicate the potential of SAR systems for thematic mapping, considering also the restrictions of frequency and polarization from each of the operational sensor systems used.

Within this frame, the objective of this work is to analyze the graphic representation of polarimetric signatures of SAR data (L-band) in primary forest, secondary succession, forests with timber exploitation and those under recovery, after a surface burning process. Additionally, another objective is an exploratory analysis of scattering mechanisms of tropical forest typology in accordance with the alternative procedure of SAR image classification based on target decomposition.

2 AREA UNDER STUDY

The area under study is located in the Tapajós region (NW Pará State, Brazil), comprised by geographical coordinates S 3º 01' 59.85" - S 3º 10' 39.33" and WGr 54º 59' 53.08" - WGr 54º 52' 44.96". This region is characterized by a low rolling relief, constituting the lower Amazon plateau and the upper Xingu-Tapajós Plateau. It is dominated by a continuous cover of primary tropical rainforest presenting on the plateaus emergent trees and an uniform vegetation cover (Dense Ombrophilous Forest), and sections of low to dissected plateaus with few emerging individuals and a high density of palm trees (Open Ombrophilous Forest). Land use is related to subsistence agriculture, few cash crops, cattle raise and selective logging activities.

3 METHODOLOGICAL APPROACH

3.1 Acquisition of airborne SAR data

The MAPSAR Project (Multi-Application Purpose SAR) is a Brazil-Germany scientific cooperation, whose initial objective was a feasibility study focussing on an L-band SAR satellite with fine spatial resolution, polarimetry and interferometry (Schroder et al. 2005). An experiment was done in the Tapajós region to simulate MAPSAR satellite data (Mura et al., 2007), using an airborne SAR-R99B sensor of SIVAM (System for the Vigilance of Amazon). SAR data were collected in September 2005, at HH, VV and HV polarizations (descending mode), with a spatial resolution of 5 m, and incidence angle varying from 52.7º to 70.1º.

The SAR data were calibrated as follows: 1^{stly} antenna pattern correction was done to remove gain variations in the range direction by a polynomial function applied to the sum of the amplitude values; and 2^{ndly} absolute calibration, based on 12 corner reflectors placed in the area under study during the imaging campaign, to allow the transformation of amplitude data in backscatter values of targets, using the method of peak power. At the absolute SAR calibration, the average error was -0.8443 dB and the standard deviation 0.18 dB.

3.2. SAR data analysis and field survey

Interaction mechanisms between SAR data and structural properties (e.g. density, shape, dielectric constant, height, biomass, etc) of the land cover are the focus of several studies, where the polarimetric signatures were used as an analysis procedure (Henderson and Lewis, 1998). According to van Zyl et al. (1987), the polarimetric signatures of targets allow a detailed knowledge of the scattering mechanisms which determine the radiation response to the SAR antenna. The scattering mechanisms can predict the backscattering coefficient, not only as a function of the incidence angle and electric properties but also considering the polarization. It is important to remind that polarimetric signatures are not the unique for a certain type of forest cover, because different combinations of distinct mechanisms of scattering could have the same signature.

In this context, an exploratory analysis was conducted to evaluate the sensitivity of two polarimetric techniques to evaluate the structural variations of some classes of forest cover. The following classes were chosen for this analysis, which was based on a field survey, done in September 2005 simultaneously with the SAR campaign: primary forest (PF), forest with old timber exploitation (SL), advanced secondary succession (ASS), intermediate secondary succession (IntSS), initial secondary succession (ISS), degraded forest (DF) by fire (occurrence of fire approximately 10 years ago). Forest inventories were done for the physiognomic-structural characterization of these typologies.

At the first analysis, a graphic representation of the parallel polarization response of six samples sections was generated, as described by Van Zyl et al. (1987). In this representation, a cross section of a certain type of forest cover (σ) is plotted on a tri-dimensional graphic, as a function of all combinations of orientation angles (ψ) and ellipticity (χ), related to the polarization ellipsis. In order to construct a polarization response of a given ROI (sample area that includes a sufficient amount of representative pixels of the theme, reducing the statistical uncertainties and the influence of the speckle noise) at the SAR image, we used an average value, at the complex format of all pixels. The resulting surfaces were compared among them by visual analysis, based on structural information obtained during forest inventory.

At the second exploratory analysis the entropy values and the average alpha angle (resulting from the decomposition of eigenvalues and eigenvectors of the coherence matrix) of the same ROIs were plotted in the bi-dimensional classification space $\left(H, \overline{\alpha}\right)$, according to a procedure introduced by Cloude & Pottier (1997). At this procedure of classification by target decomposition, the scattering mechanisms are defined at 9 distinct zones, namely: Z1- High Entropy Multiple Scattering; Z2 - High Entropy Vegetation Scattering; Z3 - High Entropy Surface Scatter; Z4 - Medium Entropy Multiple Scattering; Z5 – Medium Entropy Vegetation Scattering; Z6 – Medium Entropy Surface Scatter; Z7 – Low Entropy Multiple Scattering Events; Z-8 – Low Entropy Dipole Scattering; Z9 – Low Entropy Surface Scatter. After the inclusion of the SAR response of each ROIs into the $\left(H, \overline{\alpha}\right)$ bi-dimensional spatial classification, a statistical test based on a linear regression model (F test of b1 = 0 versus b1 ≠ 0; t test of b0 = 0 versus b0 ≠ 0; and t test of b1 = 1 versus b1 ≠ 1; b0 and b1 are the regression coefficients) was applied to verify the existence of significant differences between .classifications (combination of all possible pairs of classification derived from each ROI). The classification result is a set of 9 values in per cent, presented by a certain ROI, representing the amount of pixels classified in each zone of the plan $\left(H, \overline{\alpha}\right)$.

4 RESULTS AND DISCUSSION

At Figure 1 the responses of parallel L-band polarization of the six ROIs are presented, which were selected to represent the diversity of the vegetation typology studied. The responses of polarization of plots ISS, IntSS and ASS show a similarity to the theoretical responses of short and thin conducting cylinders (i.e. rays at lower lengths than the wavelength). This presupposes that the scattering by twigs and small branches gives an important contribution at the total backscattered radiation from inside these regeneration classers. The highest values of **σ,** at plots ASS and IntSS occur at linear polarizations ($\chi = 0°$), with preferentially horizontal orientation ($\psi = \pm\ 90°$). Taking into account that these are younger recovery areas, it is probable that the radar response was derived from more homogeneous canopies with low species diversity, where most branches are oriented horizontally. On the other hand, the representative plot of the ASS typology also presents higher values of **σ**; however at linear polarizations the response indicates the predominance of branches oriented at - 45º as related to the horizontal. When advancing at the succession stage, the vertical structure becomes more complex as well as the diversity of species, implying at an increase of the pedestal (which represents the non-polarized component) of the polarimetric signature.

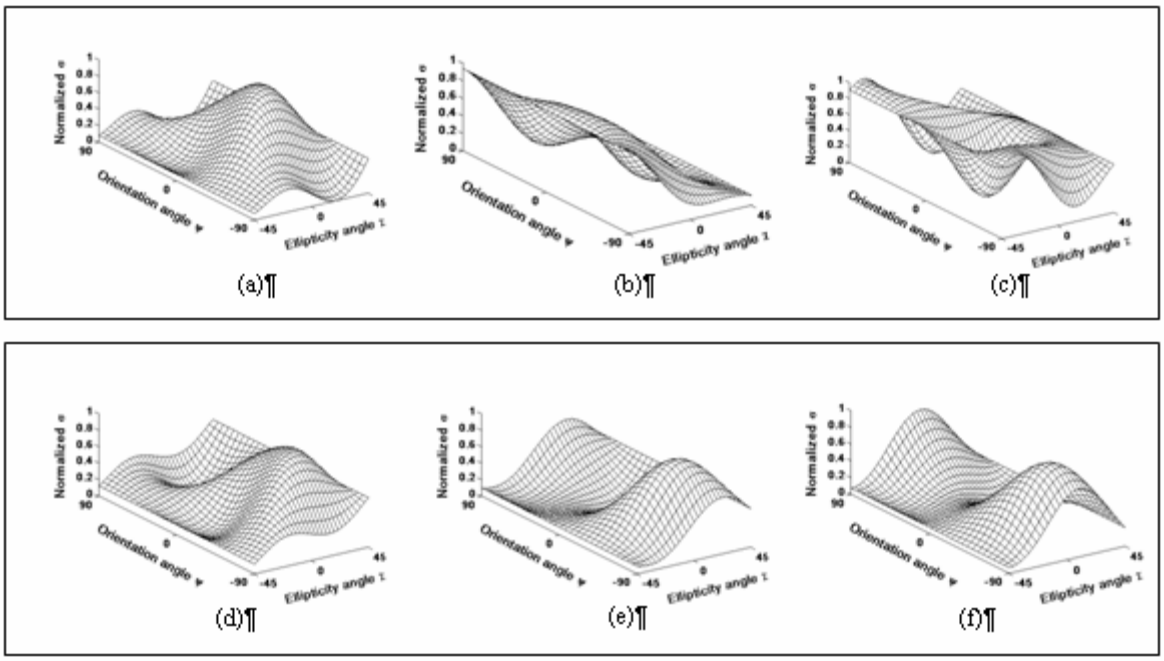

Figure 1. Polarimetric signature at band L of (a) degraded forest, (b) primary forest , (c) forest with old selective logging, (d) advanced secondary succession, (e) intermediate secondary succession and (f) initial secondary succession.

Observing Figure 1 one denotes that the L-band polarimetric signature of primary forest (PF) is similar to the theoretical response of a helix oriented to the right. The highest values of σ occur at circular RR polarization, at a certain independence from the orientation angle. In the case of plot DF, the scattering by branches presents an important contribution at the total backscattered, as it is the case with the ROIs of secondary succession, since this forest typology, after a fire incidence a long time ago, has at its low strata a component of the recovery species, competing for light with its branches oriented more vertically, amid the under-growth with thin bamboos. The polarization response is similar to the theoretical response of short and thin conducting cylinders, but in this case with a preferential vertical orientation.

In case of the representative plot of the class SL (with selective logging in 2001), the polarization response is very similar to that one observed by rotational trihedral corner reflectors which have a double bounce scattering geometry, when one of the reflector sides is aligned with the direction of electromagnetic radiation, as mentioned by Zebker and Norikane (1987). So the dominant scattering is of double bounce type, which is the reason of the larger number of gaps resulting from cutting some trees with commercial value and also because this type of mature forest has a well-defined vertical structure in various strata with a much more thin undergrowth. It is important to remark that the polarization response of this section presented a relatively high pedestal, suggesting that there is a significant variation of the scattering properties at elements of adjacent resolutions. This must be due to the influence of gaps, a consequence of selective logging which causes an increase at the structural heterogeneity.

At Figure 2 the distribution of pixels of the six ROIs can be seen at the two-dimensional classification space, whose classification results and the respective values in percent, by scattering zone, can be observed at Table 1. At Figure 2 one observes that all 6 ROIs show a concentrated pixel distribution (average value of 91.6%) at zones Z5, Z4 and Z6. This indicates that at the plots sampled, those scattering processes of medium entropy predominate and at an overview, it is independent of the floristic composition and structural characteristics of each forest typology studied. Only in those cases of primary forest and of forest degraded by fire, the amount of classified pixels, in the three zones mentioned, is below 90%. It is also important that the proportions of pixels for each zone were similar for most ROIs, except at those plots of degraded forest and at initial secondary succession. At these two cases, zone Z5 surpasses ~1.7 times the percentage of zone Z4, indicating that in these two vegetation typologies there is less multiple scattering, if compared to the other classes under study.

The statistical tests used to detect variations among classifications of pairs of ROIs, at 5% significance values, indicate that there are no significant differences. We observed larger ***p*** values at the comparison DF/PF, ISS/SL and IntSS/SL, with values of 0.964, 0.909 and 0.816 respectively, while the other ROIs were classified in equivalent mode, presenting low ***p*** values. Since there are floristic differences in primary forest areas and those at successional stages, one can infer that, at this level of significance, this classification procedure $(H, \overline{\alpha})$ by target decomposition was not enough robust to detect such a variability.

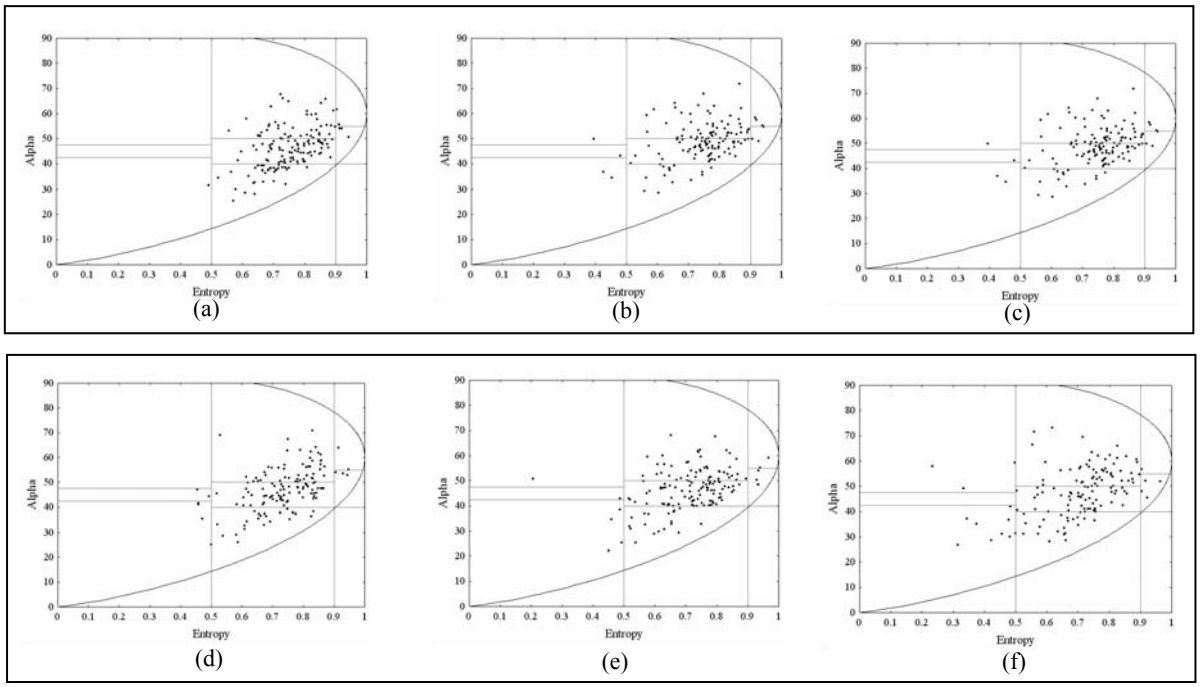

Figure 2. L-band MAPSAR α-H distribution for scattering mechanism: (a) degraded forest, (b) primary forest, (c) forest with old selective logging ,(d) advanced secondary succession , (e) intermediate secondary succession, (f) initial secondary succession.

Zones*	ROIs (Vegetation types)					
	PF	DF	SL	ASS	IntSS	ISS
Z1	0.7	1.0	1.0	1.1	1.8	0.9
Z2	2.8	1.7	2.5	1.8	2.6	1.8
Z3	0.0	0.0	0.0	0.0	0.0	0.0
Z4	37.2	26.2	32.1	34.4	40.5	28.7
Z5	32.5	49.1	46.6	43.8	40.7	46.4
Z6	19.8	11.9	13.3	14.8	10.4	21.1
Z7	1.3	1.3	0.4	0.0	1.0	0.0
Z8	0.0	0.9	0.9	1.4	1.0	0.0
Z9	5.7	7.7	3.2	2.6	2.1	1.0

Table 1. Percent pixel distribution of each ROI at zones of two-dimensional classification space $(H, \overline{\alpha})$.

5 CONCLUSIONS

The analysis of airborne SAR-R99B data (L-band) based on the classification by target decomposition supported by information derived from forest inventories, allow the following conclusions: (a) at types of landscapes studied there is a predominance of scattering processes with medium entropy. The three main scattering mechanisms observed at the experiment, in decreasing order of occurrence are: dipole, double bounce and surface type; (b) the classification method by target decomposition based on entropy values and of the average alpha angle was not robust enough to detect the floristic-structural variability existing among certain land cover classes; (c) the parallel polarization responses obtained from several forest cover classes present different configurations, indicating that the backscatter of certain plots was dominated by distinct physical mechanisms. The floristic arrangement, the diameter distribution and the height of trees isolated do not determine these polarization responses. Additional studies must be made which would allow the analysis of the spatial distribution effect of trees within the entire section and its relation with the polarimetric signature as well as the interaction mechanisms.

REFERENCES

Cloude, S. R.; Pottier, E., 1997. An entropy based classification scheme for land application of polarimetric SAR. *IEEE Transactions on Geoscience and Remote Sensing,* 35(1), pp. 68-78.

Hendersen, F.M.; Lewis, A.J., 1998. Radar fundamentals: The geoscience perspective. In: Ryerson, R.A. ed., Principles & Applications of Imaging Radar. *Manual of Remote Sensing*, 3. ed. New York, John Wiley & Sons, Inc., v.2, cap.3, p.131-181.

Hoekman, D. H.; Quinones, M. J., 2000. Land cover type and biomass classification using AirSAR data for evaluation of monitoring scenarios in the Colombian Amazon, *IEEE Transactions Geoscience and Remote Sensing*, 38 (2), pp.685–696.

Kugler, F.; Papathanassiou, K.P.; Hajnsek, I., 2006. Forest height estimation over tropical forest by means of polarimetric SAR interferometry. In: *Seminário de Atualização em Sensoriamento Remoto e Sistemas de Informações Geográficas Aplicados à Engenharia Florestal*, 7., Curitiba, Paraná, 17-19 out., 2006. Anais. pp.504-512. [CDROM].

Mura, J.C., Paradella, W.R., Dutra, L.V., 2007. MAPSAR image simulation based on L-band polarimetric SAR of the airborne SAR R99 sensor of the CENSIPAM. In *Annals of the XIII Brazilian Remote Sensing Symposium, Florianópolis, Brazil*, 2007, INPE (Ed.), pp.4943 - 4949.

Neeff, T. ; Dutra, L. V. ; Santos, J. R.; Freitas, C. C.; Araujo, L.S., 2005. Power spectrum analysis of SAR data for spatial forest characterization in Amazonia, *International Journal of Remote Sensing*, 26(13), pp. 2851-2865.

Rauste, Y.; Hame, T.; Pulliainen, J.; Heiska, K.; Hallikainen, M., 1994. Radar based forest biomass estimation, *International Journal of Remote Sensing*, 15(14), pp. 2797-2808.

Saatchi, S.S.; Soares, J.V.; Alves, D.S., 1997. Mapping deforestation and land use in Amazon rainforest by using SIR-C Imagery. *Remote Sensing of Environment*, 59(2), pp. 191-202.

Santos, J.R.; Freitas, C.C.; Araujo, L.S.; Dutra, L.V.; Mura, J.C.; Gama, F.F.; Soler, L.S.; Sant'Anna, S.J.S., 2003. Airborne P-band SAR applied to the aboveground biomass studies in the Brazilian tropical rainforest, *Remote Sensing of Environment*, 87(4), pp.482-493.

Schroder, R., Puls, J., Hajnsek, I., Jochim, F., Neeff, T., Kono, J., Paradella, W.R., Silva, M.M.Q., Valeriano, D.M., and Costa, M.P.F., 2005. MAPSAR: a small L-band SAR Mission for Land Observation. *Acta Astronautica*, 56, 35 - 43.

Treuhaft, R.N.; Chapman, B.; Dutra, L.V.; Gonçalves, F.G.; Santos, J.R.; Mura, J.C.; Graça, P.M.L.A.; Drake, J., 2006. Estimating 3-dimensional structure of tropical forest from radar interferometry, *Ambiência*, 2(1), pp. 111-119.

van Zyl, J. J., Zebker H.A., Elachi C., 1987. Imaging radar polarimetric signatures: theory and observation. *Radio Science*, 22(4), pp. 529-543.

Zebker, H.A.; Norikane, L., 1987. Radar polarimeter measures orientation of calibration corner reflectors. In: *Proceedings of the IEEE*, vol. 75, pp. 1686-1688.

ACKNOWLEDGEMENTS

The authors acknowledge to CNPq, CAPES and FAPESP for the research grants; the CENSIPAM, IBAMA/MMA and LBA for the logistic support in this study.